Proc. Natl. Acad. Sci. USA
Vol. 88, pp. 6731–6735, August 1991
Medical Sciences

Expression of the human apolipoprotein A-I gene in transgenic mice alters high density lipoprotein (HDL) particle size distribution and diminishes selective uptake of HDL cholesteryl esters

TOVA CHAJEK-SHAUL*, TONY HAYEK, ANNEMARIE WALSH, AND JAN L. BRESLOW

Laboratory of Biochemical Genetics and Metabolism, The Rockefeller University, 1230 York Avenue, New York, NY 10021-6399

Communicated by Alexander G. Bearn, April 15, 1991

ABSTRACT **Transgenic mice carrying the human apolipoprotein (apo) A-I gene (HuAITg mice) were used to examine the effects of overexpression of the human gene on high density lipoprotein (HDL) particle size distribution and metabolism. On a chow diet, control mice had HDL cholesterol and apo A-I levels of 49 ± 2 and 137 ± 12 mg/dl of plasma, respectively. HuAITg mice had HDL cholesterol, human apo A-I, and mouse apo A-I levels of 88 ± 2, 255 ± 19, and 16 ± 2 mg/dl, respectively. Nondenaturing gradient gel electrophoresis revealed control mouse plasma HDL to be primarily monodisperse with a particle diameter of 10.2 nm, whereas HuAITg mouse plasma HDL was polydisperse with particles of diameter 11.4, 10.2, and 8.7 nm, which correspond in size to human HDL_1, HDL_2, and HDL_3, respectively. *In vivo* turnover studies of HDL labeled with [^{3}H]cholesteryl linoleyl ether (representing the cholesteryl ester pool) and ^{125}I-apo A-I were performed. In control animals, the fractional catabolic rate (FCR) for HDL cholesteryl ester (0.197 ± 0.010 pool/hr) was significantly ($P < 0.0005$) more than the apo A-I FCR (0.118 ± 0.006 pool/hr). In the HuAITg mice, the HDL cholesteryl ester FCR (0.124 ± 0.008 pool/hr) was the same as the apo A-I FCR (0.126 ± 0.010 pool/hr). There were no significant differences between control and HuAITg animals in the sites of tissue removal of HDL cholesteryl ester, with the liver extracting most of the injected radioactivity. Control and HuAITg animals had comparable liver and intestinal cholesterol synthesis and LDL FCR. In conclusion, HuAITg mice have principally human and not mouse apo A-I in their plasma. This apparently causes a change in HDL particle size distribution in the transgenic mice to one resembling the human pattern. The replacement of mouse by human apo A-I also apparently causes the loss of the selective uptake pathway of HDL cholesteryl esters present in control mice. These data imply that apo A-I primary structure has a profound influence on HDL particle size distribution and metabolism.**

High density lipoproteins (HDLs) are macromolecular complexes of protein and lipid that range in diameter from 70 to 100 Å and in mass from 200 to 400 kDa. In humans, there are two major populations of HDL, a lighter one (1.063–1.12 g/ml) called HDL_2 and a heavier one (1.12–1.21 g/ml) called HDL_3. HDLs contain, on the average, 50% lipid and 50% protein. The lipid is 32% cholesteryl esters, 5% free cholesterol, 55% phospholipid, and 8% triacylglycerol. The protein consists principally of apolipoprotein (apo) A-I (70%) and apo A-II (20%). HDL metabolism is complex. Nascent HDL produced by liver and small intestine consist of apo A-I/phospholipid complexes. These attract excess free cholesterol from extrahepatic cells and other lipoproteins. This cholesterol is esterified in plasma by the lecithin–cholesterol acyltransferase, which uses apo A-I as a cofactor. The cholesteryl ester produced shifts to the core of the HDL and enlarges its size. In humans, HDL particles can also become smaller when the cholesteryl ester transfer protein (CETP) exchanges cholesteryl ester in HDL for triacylglycerol in very low density lipoprotein (VLDL) and low density lipoprotein (LDL), and then hepatic lipase hydrolyzes HDL triacylglycerols and phospholipids. In normal humans, two-thirds of the HDL exists as HDL_3 and one-third as HDL_2 (1, 2).

Because low HDL cholesterol levels are a strong risk factor for coronary heart disease (3) and because nascent HDL attracts free cholesterol from cells, it has been postulated that HDL participates in a reverse cholesterol transport pathway. In this pathway, excess free cholesterol in extrahepatic cells is removed by HDL, esterified, and transported back to the liver for excretion (4). Evidence has been presented for three mechanisms for this to occur: (*i*) the uptake of whole HDL particles by the liver (5), (*ii*) the selective uptake of HDL cholesteryl esters as distinct from particulate uptake (6, 7), and (*iii*) the transfer of HDL cholesteryl esters by CETP to apo B-containing particles, which are removed by liver LDL receptors (8, 9).

We have described a transgenic mouse model that expresses the human apo A-I gene (10). Human apo A-I was incorporated into HDL, and plasma HDL cholesterol was directly proportional to human apo A-I expression. In the current study, we used these mice to examine the effects of increasing plasma apo A-I and HDL cholesterol on HDL metabolism. These transgenic mice underexpress mouse apo A-I, with most apo A-I in plasma being human. As a result, we noted a change in HDL, from primarily monodisperse in control mice to polydisperse with a pattern like that of human HDL occurring in the transgenic mice. The selective uptake pathway of HDL cholesteryl esters readily demonstrated in control mice could not be demonstrated in the transgenic mice. These experiments show that apo A-I primary structure has a profound influence on HDL particle size distribution and metabolism.

MATERIALS AND METHODS

Animals. We previously described five lines of human apo A-I-transgenic (HuAITg) mice (10). The line with the highest level of human apo A-I expression, Tg 427, was used for the current studies. Transgenic animals were (C57BL/6J × CBA/J)F_1. These were mated with the same F_1 nontransgenic mice, and transgenic and nontransgenic littermates were compared in the current study. The mice were used for metabolic studies at ≈8 weeks of age (weight, 24–30 g). They

The publication costs of this article were defrayed in part by page charge payment. This article must therefore be hereby marked "*advertisement*" in accordance with 18 U.S.C. §1734 solely to indicate this fact.

Abbreviations: HDL, high density lipoprotein; LDL, low density lipoprotein; VLDL, very low density lipoprotein; apo, apolipoprotein; CETP, cholesteryl ester transfer protein; FCR, fractional catabolic rate.

*Permanent address: Department of Medicine, Lipid Research Laboratory, Hadassah Hospital, Jerusalem, Israel.

Table 1. Levels of HDL cholesterol (Chol) and apo A-I and fractional catabolic rates (FCRs) of HDL cholesteryl esters (CE) and apo A-I

Diet	Mice	Level, mg/dl			FCR, pool/hr	
		HDL Chol	Human A-I	Mouse A-I	HDL CE	A-I
Chow	Control	49 ± 2	—	137 ± 12	0.197 ± 0.010†	0.118 ± 0.006
	HuAITg	88 ± 6	255 ± 19	16 ± 2	0.124 ± 0.008	0.126 ± 0.01
High fat	Control	86 ± 4*	—	196 ± 10*	0.170 ± 0.010†	0.094 ± 0.006
	HuAITg	137 ± 8*	349 ± 13*	51 ± 9*	0.108 ± 0.009	0.110 ± 0.01

Results are means ± SEM of 6–21 mice from 2–5 experiments.
*$P < 0.005$ when compared to its control on a chow diet.
†$P < 0.0005$ when compared to apo A-I FCR of the same group.

were caged in an animal room with a 12-hr light (7 a.m. to 7 p.m.)/dark (7 p.m. to 7 a.m.) cycle. The mice had free access to food and water.

Diet. For most experiments, the mice were fed a regular mouse chow diet (Purina Chow containing 4% fat). In certain experiments, a high-fat (40% of calories), low-cholesterol (<0.002 mg/1000 kcal; 1 kcal = 4184 J) diet was used for 3 weeks. This diet was mixed and pelleted by Teklad Premier Laboratory (Madison, WI) (TD88333). The diet contained (per kg) protein, 19 g; DL-methionine, 3 g; sucrose, 341.46 g; corn starch, 151.1 g; olive oil, 19.2 g; palm oil, 188.8 g; egg yolk powder, 3.4 g; cellulose fiber, 50 g; mineral mix AIN-76 (170915), 35 g; calcium carbonate, 4 g; vitamin mix (Teklad 40060), 10 g; ethoxyguen (antioxidant), 0.04 g.

Preparation of HDL Labeled in the Apo A-I and Cholesteryl Ester Moieties. Human apo A-I was purified and radiolabeled with ^{125}I by a modification (11) of the McFarlane method (12). Serum from control or HuAITg mice was incubated with [^3H]cholesteryl linoleyl ether (specific activity, 46.6 Ci/mmol; Amersham; 1 Ci = 37 GBq), labeled intralipid, and a rabbit plasma fraction of density > 1.25 g/ml (a source of CETP) for 16 hr at 37°C as described (13). The labeled HDL fraction was isolated by sequential ultracentrifugation between densities 1.063 and 1.21 g/ml, dialyzed against five changes of 1 liter of 0.9% NaCl/1 mM EDTA over 20 hr, and used immediately. ^{125}I-labeled apo A-I was mixed with the [^3H]cholesteryl linoleyl ether-labeled HDL prior to injection. This procedure was associated with a >90% recovery of the [^3H]cholesteryl linoleyl ether in the plasma (13) 10 min after its injection.

***In Vivo* HDL Turnover Studies.** Mice were injected (femoral vein) with either control or HuAITg mouse HDL doubly labeled with human ^{125}I-apo A-I and [^3H]cholesteryl linoleyl ether. The injected HDL mass was <5% of the mouse HDL pool. Blood (50 μl) was taken from the retroorbital plexus under anesthesia with methoxyflurane at the indicated time intervals for determination of radioactivity. The fractional catabolic rates for apo A-I and HDL cholesteryl linoleyl ether were calculated from the plasma decay curves assuming a two-pool model by the Matthews method (14). At the end of some experiments, the tissue distribution of the [^3H]cholesteryl linoleyl ether radioactivity was determined by perfusing the mice through the abdominal aorta with 50 ml of phosphate-buffered saline (pH 7.4) preheated to 37°C. Organs were then taken and homogenized in chloroform/methanol (1:1, vol/vol) and ^3H was determined.

Preparation of Radiolabeled Mouse LDL and *in Vivo* LDL Turnover Studies. Mouse LDL was isolated by sequential ultracentrifugation between 1.019 and 1.063 g/ml, dialyzed against five changes of 1 liter of 0.9% NaCl/1 mM EDTA over 20 hr, and radiolabeled with ^{125}I (11, 12). LDL turnover was assessed as above for HDL.

***In Vivo* Sterol Synthesis.** One hour after i.p. injection of ^3H_2O (Amersham), mice were exsanguinated through the heart and incorporation of ^3H_2O into tissue cholesterol was determined (15).

Apo A-I Quantitation. Human apo A-I was quantitated by a sandwich ELISA using a goat polyclonal anti-human apo A-I antibody that had <0.01% crossreactivity with mouse apo A-I (10). Mouse apo A-I was quantitated by "rocket" electroimmunoassay using a polyclonal anti-mouse apo A-I antibody prepared in cynomolgus monkeys and generously supplied by George Melchior (Upjohn). This antibody had <0.01% crossreactivity with human apo A-I.

Plasma Lipid and Lipoprotein Analysis. Total cholesterol was determined enzymatically using the Boehringer Mannheim reagents. HDL cholesterol was determined after precipitation of apo B-containing lipoproteins by dextran sulfate (10). Nondenaturing gradient get electrophoresis in 4–30% polyacrylamide gels (Pharmacia) was performed to determine HDL particle size (16, 17).

RESULTS

Control and HuAITg mice manifest different HDL cholesterol concentrations (Table 1). On a chow diet, the average control animal HDL cholesterol is 49 ± 2 mg/dl and the transgenic 86 ± 4 mg/dl. This is reflected in different levels of apo A-I. The average control animal apo A-I is 137 ± 12 mg/dl and the transgenic 271 ± 19 mg/dl. Of course, control animals have only mouse apo A-I, whereas in transgenic animals 90% of the apo A-I is human. Nondenaturing gradient gel electrophoresis revealed control mouse plasma HDL to be monodisperse with a diameter of 10.2 nm, whereas HDL in the HuAITg mouse plasma was polydisperse with major populations of particles of diameters 8.7, 10.2, and 11.4 nm (Fig. 1). Western immunoblotting analysis of the gradient gel revealed the presence of both human and mouse apo A-I in all HuAITg mouse HDL subfractions (data not shown).

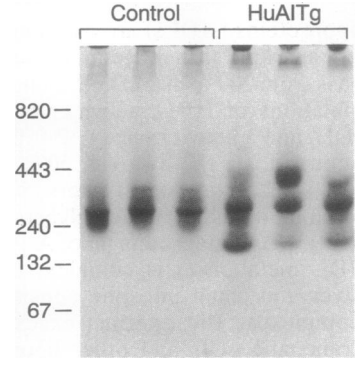

FIG. 1. Nondenaturing gradient gel electrophoresis of control and HuAITg mouse plasma. Plasma samples (25 μl) were stained with Sudan black prior to electrophoresis in a native 4–30% polyacrylamide gradient gel. Lipid-stained lipoproteins were detected in control and HuAITg mouse plasma. Molecular size markers (kDa) are indicated at left.

Utilizing HDL labeled in the apo A-I and cholesteryl ester moieties, we next examined the disappearance rates of these HDL components from plasma in control and HuAITg animals. We first showed that both tracers adequately label HDL in control and HuAITg mice. Fig. 2 shows that ^{125}I-apo A-I and [^{3}H]cholesteryl linoleyl ether are each associated with the single HDL fraction from control animals and all HDL fractions from the transgenics. Fig. 3 shows the plasma decay curves after injection of doubly labeled control or transgenic HDL into control animals. In the control animals the disappearance rate of [^{3}H]cholesteryl linoleyl ether was significantly greater than that of ^{125}I-apo A-I. In contrast, when doubly labeled control or transgenic HDL was injected into HuAITg animals, the disappearance rates of the [^{3}H]-cholesteryl linoleyl ether and ^{125}I-apo A-I were identical (Fig. 4). From the plasma decay curves, the FCRs were calculated (Table 1).

The decrease of HDL cholesteryl ether FCR in HuAITg mice compared with controls could either reflect a metabolic difference between the HDL particles or be the result of the increased level of HDL cholesterol observed in HuAITg mice causing saturation of a removal pathway. To address this issue, we fed control and HuAITg mice a high-fat, low-cholesterol diet, which increased the control HDL cholesterol to the level of the HuAITg animals on chow (Table 1). Even at these elevated HDL cholesterol levels, the control

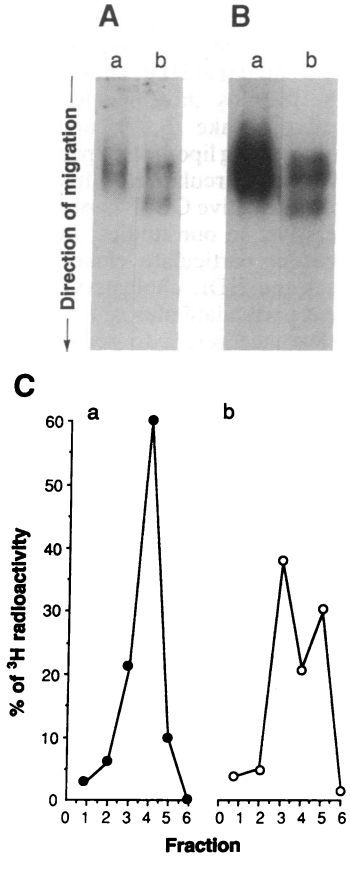

FIG. 2. [^{3}H]Cholesteryl linoleyl ether-labeled HDL from control or HuAITg mice was mixed with ^{125}I-human apo A-I, stained with Sudan black, and electrophoresed in a native 3–17% polyacrylamide gradient gel. The Sudan black pattern (*A*) and the autoradiogram (*B*) show that the ^{125}I-apo A-I radioactivity is associated with the single HDL fraction in control mice (lane a) and all HDL subfractions in HuAITg animals (lane b). The percentage of ^{3}H radioactivity (*C*) in several slices of the HDL bands taken from the gel shows that [^{3}H]cholesteryl ether is associated with the single HDL fraction in control animals (plot a) and all HDL subfraction in HuAITg animals (plot b).

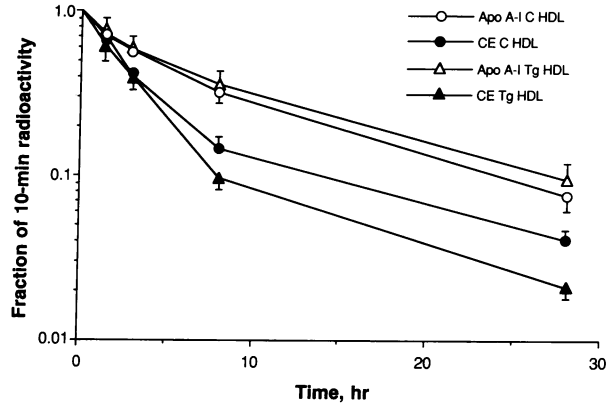

FIG. 3. Plasma radioactivity decay curves of doubly radiolabeled HDL in control mice (n = 29). Control mice were injected i.v. with ^{125}I-labeled human apo A-I mixed with [^{3}H]cholesteryl linoleyl ether (CE)-labeled control (C) or transgenic (Tg) HDL. Blood (50 μl) was taken from the retroorbital plexus at the indicated time for determination of radioactivity.

animals showed a similar increase in the HDL cholesteryl ether FCR compared with apo A-I FCR. Thus, high HDL cholesteryl ester by itself is not responsible for the loss of the rapid clearance of HDL cholesteryl ether. Rather, a metabolic difference must exist between the control and the HuAITg particles.

The clearance of [^{3}H]cholesteryl linoleyl ether by various organs was next examined and shown to be similar between control and HuAITg mice (Table 2). The liver extracted most of the injected radioactivity, whereas the adrenals were the most active on a per-gram-of-tissue basis. Thus the metabolic fate of the HDL cholesteryl ether is unchanged. Cholesterol synthesis rates and LDL turnover in liver and small intestine were examined next. Control and HuAITg animals showed similar diurnal variation and dietary fat suppression of cholesterol synthesis (Table 3). LDL turnover studies were also performed using ^{125}I-labeled mouse LDL and no differences between control and HuAITg mice were observed (Fig. 5).

DISCUSSION

The introduction of the human apo A-I gene into mice by transgenic technology has allowed new insights into HDL metabolism. In the current study we show that overexpression of human apo A-I is accompanied by increased HDL cholesterol levels, a change in HDL particle size distribution,

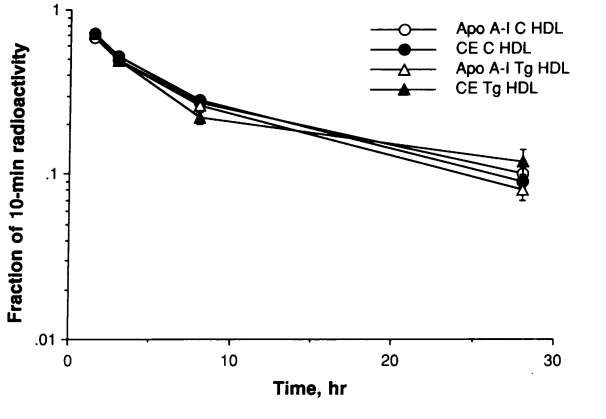

FIG. 4. Plasma radioactivity decay curves of doubly radiolabeled HDL in HuAITg mice (n = 27). HuAITg mice were injected i.v. with ^{125}I-labeled human apo A-I mixed with [^{3}H]cholesteryl linoleyl ether (CE)-labeled control (C) or transgenic (Tg) HDL. Blood (50 μl) was taken from the retroorbital plexus at the indicated time for determination of radioactivity.

Table 2. Tissue uptake of [^{3}H]cholesteryl linoleyl ether-labeled HDL

Mice	Liver	Adrenal	Kidney	Testis	Small intestine
		% of injected dose per gram of tissue			
Control	74 ± 5.7	122 ± 16	5.0 ± 0.8	3.8 ± 0.5	7.5 ± 0.9
HuAITg	63 ± 3.1	75 ± 12	4.5 ± 0.6	5.8 ± 1.4	5.5 ± 1.0
		% of injected dose per organ			
Control	62 ± 7.4	0.5 ± 0.04	1.1 ± 0.2	0.4 ± 0.04	5.4 ± 1.0
HuAITg	52 ± 2.5	0.4 ± 0.04	1.0 ± 0.6	0.3 ± 0.03	3.4 ± 0.8

Results are means ± SEM of 8–10 mice.

and a decrease in HDL cholesteryl ether FCR. However, there was no change in the tissue distribution of the HDL cholesteryl ethers, cholesterol synthesis in liver and small intestine, or LDL FCR. These studies strongly suggest that apo A-I primary structure (i.e., human vs. mouse) determines important aspects of HDL size and metabolism.

Overexpression of the human apo A-I gene in transgenic mice, presumably due to copy number, can result in high levels of human apo A-I in the plasma of these animals (10). Two previous transgenic lines were described in which this was the case. The Tg 179 line had an average human apo A-I concentration of 245 mg/dl and the Tg 427 line had 339 mg/dl. Normal levels of apo A-I in human plasma are 125–150 mg/dl. In our previous work, we could only estimate the concentration of mouse apo A-I in the plasma of the transgenic animals and concluded it was not significantly reduced (10). We have now obtained an antibody specific for mouse apo A-I and, using this for quantitation, have observed a profound decrease in mouse apo A-I concentration in the plasma of transgenic animals. In fact, mouse apo A-I in transgenic plasma is so low in concentration that ≈90% of the plasma pool is human apo A-I. Recently, Ishida *et al.* (18) have made transgenic mice by similar techniques and have reported the same observation.

In the HuAITg animals, there has been a striking change in the HDL particle size distribution. On nondenaturing gradient gel electrophoresis, HDL in control animals is monodisperse with the major peak at 10.2-nm diameter, whereas HDL in transgenic animals is polydisperse with major peaks at 11.4, 10.2, and 8.7 nm. This distribution is quite comparable to the major HDL species in humans and corresponds to HDL_1, HDL_2, and HDL_3. In our original study (10), we attempted nondenaturing gradient gel analysis to show that human apo A-I was distributed throughout the HDL size classes in the transgenic animals. In figure 7 of that publication, polydispersity of transgenic HDL compared with control mouse HDL is apparent. Ishida *et al.* (18) also reported the difference in particle size distribution between control and HuAITg mouse HDL. Thus, the primary sequence of apo A-I plays a major role in determining HDL particle size.

Overexpression of apo A-I in HuAITg animals causes a primary increase in HDL cholesterol levels. Effects on the other lipoproteins and on the metabolic state of the host are minimal (10). This is in contrast to other HDL-raising or -lowering perturbations used to date. Thus, the HuAITG mouse is a particularly appealing model to study the isolated effects of increased HDL cholesterol levels on HDL metabolism and tissue cholesterol homeostasis. By using doubly labeled HDL, we were able to assess the FCR of its apo A-I and cholesteryl ester moieties in control and HuAITg animals. We observed that the apo A-I FCR was virtually the same in both types of animals, whereas the HDL-CE FCR diminished by 40% in the HuAITg animals compared with controls. This decrease resulted in identical FCRs for both apo A-I and HDL-CE in the HuAITg mice.

These observations build on previous studies of HDL cholesteryl ester metabolism in various animal models. Evidence has been presented that HDL cholesteryl esters can be transported to the liver by three mechanisms: particulate uptake (5), selective uptake (6, 7), and CETP-mediated transfer to apo B-containing lipoprotein particles (8, 9), which can be removed from the circulation by liver LDL receptors. Since mice do not have active CETP in plasma (19), the third pathway is inoperative. In our studies, the apo A-I FCR is assumed to represent particulate clearance (whole HDL particles), whereas the HDL cholesteryl ester FCR is assumed to represent particulate plus selective clearance. The term selective clearance refers to removal of HDL cholesteryl esters without whole particle removal (6, 7). The difference between the A-I FCR and the HDL cholesteryl ester FCR represents selective clearance. We found that apo A-I FCR was the same in control and HuAITg mice in spite of the larger pool in the latter, implying that in this concentration range particulate clearance is not saturated. The HDL cholesteryl ester FCR was 40% less in HuAITg mice compared with controls and was identical to the apo A-I FCR. This suggests that the selective HDL cholesteryl ester clearance pathway present in control animals is missing or greatly diminished in the transgenic mice. This implies that the primary sequence of apo A-I determines the selective uptake

Table 3. Rates of cholesterol synthesis in liver and small intestine of control or HuAITg mice under various conditions

Diet	Mice	"Time"	Incorporation of ^3H_2O into cholesterol, μmol/hr per gram of tissue (*n*) Liver	Intestine
Chow	Control	Midday	3.0 ± 0.19 (29)	1.4 ± 0.07 (26)
	Control	Midnight	1.6 ± 0.07 (7)*	0.6 ± 0.08 (8)*
	HuAITg	Midday	2.9 ± 0.22 (18)	1.5 ± 0.05 (16)
	HuAITg	Midnight	1.5 ± 0.15 (11)*	0.6 ± 0.12 (4)*
High fat	Control	Midday	1.0 ± 0.11 (7)†	1.3 ± 0.1 (7)
	HuAITg	Midday	1.3 ± 0.08 (6)†	1.2 ± 0.07 (6)

Mice were caged in reverse light/dark cages with a 12-hr light/dark cycle for 2 weeks prior to the experiments. Cages were dark from 3 a.m. to 3 p.m. and light from 3 p.m. to 3 a.m. or vice versa. ^3H_2O was injected between 9:30 and 11:30 a.m. Results are means ± SEM of *n* mice.

*$P < 0.0005$ when compared to midday values.

†$P < 0.0005$ when compared to midday values of mice on low-fat (chow) diet.

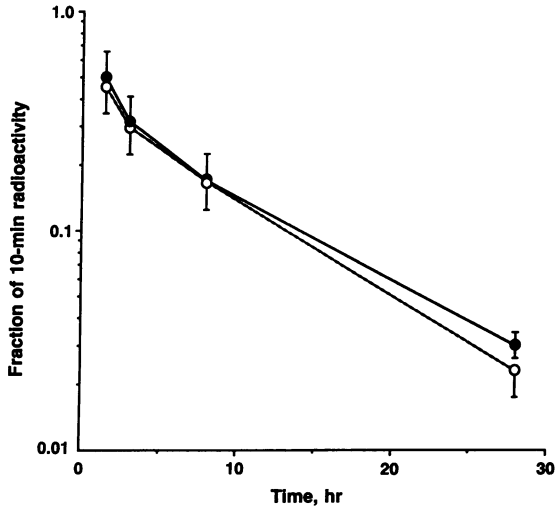

FIG. 5. Plasma radioactivity decay curve of labeled LDL. Control (n = 4) and HuAITg (n = 4) mice were injected intravenously with ^{125}I-labeled mouse LDL. Blood (50 μl) was taken from the retroorbital plexus at the indicated time for determination of radioactivity.

of HDL cholesteryl esters. It is not clear whether this is due to a protein–protein interaction (e.g., between liver membrane proteins and mouse as opposed to human apo A-I) or due to the different physical properties of HDL in control and transgenic animals. The polydispersity of HDL in the HuAITg mice may allow the HDL cholesterol esters to remain in plasma rather than be selectively transferred to the liver.

Goldberg *et al.* (20) have quantified the pathways for cellular uptake of HDL cholesteryl esters in rabbits. Based on the disappearance curve of radiolabeled HDL cholesteryl ether from plasma and on complex modeling, they concluded that 10% of the clearance was by particulate uptake, 20% by selective uptake, and 70% by CETP-mediated transfer to LDL and VLDL. Rabbits have a very high level of plasma CETP activity compared with humans. Therefore, Goldberg *et al.* suggested that since this pathway competes with the selective uptake pathway, the latter may play a substantial role in humans in the clearance of HDL cholesteryl esters. Our results suggest that human apo A-I may not allow the selective uptake pathway to operate and that clearance of HDL cholesteryl esters in humans may be divided between the particulate uptake and CETP-mediated pathways.

The consequences of the increased HDL cholesterol for deposition of HDL cholesteryl esters in tissue, for cholesterol synthesis in liver and intestine, and for the FCR of LDL were also evaluated. The increase in HDL cholesterol, the change in its particulate distribution, and the alteration in the HDL cholesteryl ester selective uptake pathway did not change the organ distribution of HDL cholesterol esters at the end of the metabolic study. The major site of removal was the liver, as has been seen by others in nontransgenic animal studies (6). Similarly there was also no difference between control and HuAITg animals in liver and intestinal cholesterol synthesis and LDL FCR. This implies that the total turnover of HDL cholesterol esters and thereby plasma cholesteryl esters (in the mouse most plasma cholesterol is in HDL cholesteryl ester) is the same in control and HuAITg mice despite the elevation of HDL cholesterol levels in the transgenic mice. In fact, our turnover data are in agreement with this suggestion. The increase in the HDL cholesterol ester pool in the HuAITg animals is exactly compensated for by the decrease in the HDL cholesteryl ester FCR due to the loss of the selective transport pathway. This is true both for mice on the chow diet and for mice on the high-fat diet. Thus, raising HDL in this model may not increase the total plasma HDL cholesterol ester turnover. If this is the case, then our study provides direct *in vivo* evidence that increased HDL cholesterol levels do not necessarily result in increased reverse cholesterol transport. This does not mean that HDL may not be protective against atherosclerosis in this model. It is possible that the expanded plasma HDL pool may be protective in and of itself.

This work was supported in part by grants from the National Institutes of Health (HL33714, HL33435, and HL36461), a General Clinical Research Center Grant from the National Institutes of Health, and general support from the Pew Trust.

1. Eisenberg, S. (1984) *J. Lipid Res.* **25,** 1017–1058.
2. Tall, A. R. (1990) *J. Clin. Invest.* **86,** 379–384.
3. Gordon, D. J. & Rifkind, B. M. (1989) *N. Engl. J. Med.* **321,** 1311–1316.
4. Reichl, D. & Miller, N. E. (1989) *Arteriosclerosis* **9,** 785–797.
5. Eisenberg, S., Oschry, Y. & Zimmerman, J. (1984) *J. Lipid Res.* **25,** 121–128.
6. Glass, C. K., Pittman, R. C., Weinstein, D. B. & Steinberg, D. (1983) *Proc. Natl. Acad. Sci. USA* **80,** 5435–5439.
7. Glass, C. K., Pittman, R. C., Civen, M. & Steinberg, D. (1985) *J. Biol. Chem.* **260,** 744–750.
8. Whitlock, M. E., Swenson, T. L., Ramakrishnan, R., Leonard, M. T., Marcel, Y. L., Milne, R. W. & Tall, A. R. (1989) *J. Clin. Invest.* **84,** 129–137.
9. Brown, M. L., Inazu, A., Hesler, C. B., Agellon, L. B., Mann, C., Whitlock, M. E., Marcel, Y. L., Milne, R. W., Koizumi, J., Mabuchi, H., Takeda, R. & Tall, A. R. (1989) *Nature (London)* **342,** 448–451.
10. Walsh, A., Ito, Y. & Breslow, J. L. (1989) *J. Biol. Chem.* **264,** 6488–6494.
11. Bilheimer, D. W., Eisenberg, S. & Levy, R. L. (1972) *Biochim. Biophys. Acta* **260,** 212–221.
12. McFarlane, A. S. (1958) *Nature (London)* **182,** 53.
13. Stein, Y., Dabach, Y., Hollander, G., Halperin, G. & Stein, O. (1983) *Biochim. Biophys. Acta* **752,** 98–105.
14. Matthews, C. M. (1957) *Phys. Med. Biol.* **2,** 36–53.
15. Feingold, K. R. & Grunfeld, C. (1987) *J. Clin. Invest.* **80,** 184–190.
16. Blanche, P. J., Gong, E. L., Forte, T. M. & Nichols, A. V. (1981) *Biochim. Biophys. Acta* **665,** 408–418.
17. Verdery, R. B., Benham, D. F., Baldwin, H. L., Goldberg, A. P. & Nichols, A. V. (1989) *J. Lipid Res.* **30,** 1085–1095.
18. Ishida, B. Y., Clift, S. M., Krauss, R. M. & Rubin, E. M. (1991) *Proc. Natl. Acad. Sci. USA* **88,** 434–438.
19. Jiao, S., Cole, T. G., Kitchens, R. T., Pfleger, B. & Schonfeld, G. (1990) *Metabolism* **39,** 155–160.
20. Goldberg, D. I., Beltz, W. F. & Pittman, R. C. (1991) *J. Clin. Invest.* **87,** 331–346.